

**INVESTIGATION OF SURFACE PREPARATION
IN SUPERPLASTIC FORMED METALS**

Alex Chillman and M. Ramulu
Department of Mechanical Engineering
University of Washington
Seattle, WA

M. Hashish
Flow International Corporation
Kent, WA

ABSTRACT

In recent years, waterjets have readily emerged showing their potential over a broad range of applications. Three of these applications are inter-twined, and experimental investigations have been performed to investigate the use of waterjets in (i) coating removal, (ii) surface texturing, and (iii) subsurface modifications. However, very little is known about the jet/material behavior when ultra high pressure waterjets (> 600 MPa) are used.

In this experimental study, the use of waterjets at 600 MPa (87 ksi) were used to qualify the jet/material interactions seen during surface preparations. The investigation was focused upon the material removal mechanism observed and the subsurface modifications when removing coatings and the alpha case layer from a Super-Plastically Formed (SPF) as-exposed fine grain Ti-6Al-4V Titanium alloy. This experiment showed that the erosion mechanics, as well as the surface texture, were highly dependent on the process parameters. Also, subsurface modifications were documented, with an increased hardness seen in the shallow subsurface levels. Although a preliminary look into surface preparation at 600 MPa, this study showed very promising results that controlled removal, creating a desired surface texture, can be achieved.

1. INTRODUCTION

Researchers have investigated the benefits found when cutting with waterjet pump pressures of 600 MPa [1,2], however, very little research has been performed regarding surface preparations at these pressures. A substantial amount of research has been performed regarding the peening and surface preparation of aerospace materials at pump pressures up to 420 MPa [3-12]. Preliminary studies [13,14] have been performed regarding the benefits of 600 MPa pump pressures for waterjet surface treatments of aerospace materials, namely Ti-6Al-4V. This experimental study expands these preliminary findings to the post-processing of Super-Plastically-Formed (SPF) Ti-6Al-4V specimens.

2. TEST PROCEDURE

Testing was performed on fine grain, Super-Plastically formed Ti-6Al-4V specimens. The Ti-6Al-4V specimens are coated with a boron coating, which serves to reduce shear stresses during the Super-Plastic forming process. The initial dimensions of Specimen #1 are 41.5 mm wide by 105 mm long by 2 mm thick. The conditions used in treating this sample are given in Table 1. All runs were performed using a standard round jet nozzle. The sample runs performed on Specimen #1 (Experimental Set #1) investigated the effect of varying the traverse rate, while holding all other process parameters constant. These tests were performed as a screening process to visually inspect the generated surfaces

Initial visual inspection of the surfaces generated during the trial runs of Specimen #1 was performed, and further investigations of surface quality were suggested. A second set (Experimental Set #2) of sample runs was performed using the same surface treatment conditions, however, this time 50 passes were taken so further surface analysis could be performed.

Surface texture of the waterjet treated surfaces of Experimental Set #2 were measured using contact profilometry with a SurfAnalyzer™ 4000 profilometer (a registered trademark of Federal, an Esterline Company) and a 5 μm probe. All measurements were obtained according to ANSI B46.1-1986 using a 0.8 mm cutoff length and 3 mm traverse length. Surface profilometry was performed both parallel and perpendicular to the direction of jet traverse to verify the isotropic nature of the generated surfaces. Standard roughness parameters, including arithmetic average roughness (R_a), peak to valley height (R_y), root mean square roughness (R_q), and ten-point height (R_z) were calculated for each profile.

Sub-surface impacts of the waterjet surface treatment were detected by measuring the hardness variations that resulted. For this experimentation, hardness measurements were obtained from a polished surface. The distribution of subsurface plastic deformation was determined by analyzing the Knoop micro-hardness measurements through the depth of the cross-section perpendicular to the direction of jet traverse during the surface preparation processes.

Visual examination was performed to provide insight into the material removal methods and surface generation for the Experimental Sets. Scanning Electron Microscopy (SEM) was used to

examine the treated surfaces, and detect the surface erosion mechanics that occurred under each of the experimental conditions. The specimens were ultra-sonically cleaned, and dried using nitrogen air to avoid any contamination to the material surface by foreign particles. The surfaces of the samples were then examined using an electron beam voltage of 10 kV and magnifications of 100x, 500x, 1000x, and 2000x using the SEM.

3. RESULTS

3.1. Surface Profile

Figure 1 shows the as-prepared Experimental Set #1. These trial runs were made by varying the traverse rate from 21.2 mm/s – 169.3 mm/s with a constant pressure, standoff distance, and lateral displacement. From viewing Figure 1, it can be seen that the material was completely eroded at 21.2 mm/s, and treatment at a jet traverse rate of 169.3 mm/s did not fully remove the boron coating.

The surface generated with a 21.2 mm/s case is extremely rough in comparison to the other profiles. Figure 2 shows a comparison of the surface profiles, which was generated using contact profilometry.

The surface produced with a traverse rate of 21.2 mm/s exhibits a very un-uniform surface profile when compared to the 31.7 mm/s case, as seen in Figure 2. A further comparison of the other three surfaces (42.3, 84.7, and 169.3 mm/s traverse rates) show that very little variations in surface profiles existed. This demonstrates that a threshold traverse rate occurs somewhere between 21.2 mm/s and 31.7 mm/s, where any traverse rate lower than the threshold value will have detrimental effects on the surface leading to an undesirable degree of erosion.

Another factor of concern was the influence of jet traverse direction on the generated surface profiles. Ideally, the surface would exhibit isotropic properties, where the profile and roughness values were independent of the jet traverse direction. Surface profile measurements were performed both parallel and perpendicular to the jet traverse direction for the case of a 31.7 mm/s traverse rate, as seen in Figure 3. The surface profiles produced are similar; however the perpendicular direction shows a greater peak to valley variation.

The values of R_a , R_q , R_y , and R_z can be seen in Table 2. The results of the arithmetic average roughness evaluation with varying traverse rate can be seen in Figure 4 for the surface analysis of Experimental Set #2. It appears that traverse rates of 31.7 mm/s and greater do not have detrimental effects on the surface roughness.

3.2. SEM Surface Analysis

Scanning Electron Microscopy was performed on the surfaces of Experimental Set #1 to investigate the material removal mechanism for the different cases. Images of the treated regions can be seen in Figure 5. Clearly, a drastic transition in the surface generated can be seen as the jet traverse rate increases from 21.2 mm/s to 31.7 mm/s. When the jet traverse rate is 21.2 mm/s,

erosion is the dominant removal mechanism. None of the original surface characteristics remain, and the surface profiles show a very rugged surface, dominated by peaks and valleys. The surface generated seems to exhibit microscopic fractures, which results in an undesirable surface. As the jet traverse rate increases to 31.7 mm/s, the original surface is no longer completely eroded. Instead, isolated erosion occurs, and small pits approximately 5-8 micrometers in diameter form. This is due to a reduction in jet / material exposure time as the traverse rate increases, and a reduced number of droplets impinging on the material surface. As the traverse increases further (Figure 2.c and 2.d) it can be seen that the pockets of erosion become less prevalent on the surface, and a typically smooth surface is generated at 169.3 mm/s traverse rate.

3.3. Surface Texturing

Surface textures of Experimental Set #2 can be analyzed by evaluating statistical parameters such as surface height distribution and bearing ratio. Skewness and kurtosis can also be examined to evaluate the peaked-ness and symmetry of the surfaces generated. The bearing ratio defines the percentage of material exposed to air for the surface profiles at any constant surface level. The surface skewness defines the nature of an asymmetrical surface distribution with respect to a purely symmetric or “Gaussian” spread, while kurtosis defines the relative peaked-ness or flatness of the distribution compared with the normal distribution. A negative skewness is ideal for bearing surfaces that require large contact areas, while positive skewness is more effective in minimizing fatigue failures through free abrasive erosion.

The surface height distribution for Experimental Set #2 can be seen in Figure 6. The cases of 31.7, 42.3, 84.7, and 169.3 mm/s exhibit very similar profile height distributions. It is important to note that all of these distributions have an upward shift, with the highest percentage of exposed surface located above the centerline. The profile height distribution for the 21.2 mm/s traverse rate exhibits a very broad distribution. This broad distribution is the result of the severe erosive craters that formed, as seen in the SEM images.

The bearing curves can also be evaluated to exhibit the type of surface generated. Figure 7 shows the bearing curves of the surfaces generated parallel to the jet traverse direction. The distribution for the case of 21.2 mm/s shows a greater variation in surface heights, with nearly 40% of the surface exhibiting a height with magnitude greater than +/- 5 micrometers. It is also important to note that over ½ of the exposed surface lies above the centerline, which is typical for a water-erosion generated surface where pockets of erosion form. Finally, the cases of 31.7, 42.3, 84.7, and 169.3 mm/s exhibit very similar trends. The surfaces show very small variation in the bearing curve, but 60% of these surfaces are located above the centerline.

Experimental Set #2 skewness and kurtosis values can be evaluated. The plot of Kurtosis vs Skewness for profiles acquired perpendicular to the jet traverse direction for Experimental Set #2 can be seen in Figure 8. This plot shows that the majority of traverse rates display a negative skewness, close to zero in magnitude, which will be beneficial for bearing surfaces. This is also typical of the erosive nature of water erosion processes.

3.4. Microhardness Variations

Sub-surface modifications were evaluated with micro-hardness testing on Experimental Set #2. The hardness values were normalized against the base material Knoop hardness value. Figure 9 shows a comparison of the normalized Knoop hardness value with variable traverse rates.

The normalized Knoop hardness values seen in Figure 9 show that the 21.2 mm/s and 31.7 mm/s traverse rates related to a higher increase in the Knoop hardness value near the surface. The maximum increase seen was approximately 9% from the base material hardness value. A correlation was seen between the traverse rates such that the base material hardness value was reached at a depth of approximately 150 micrometers below the treated surface. This demonstrates the jet prepared surface's beneficial effects.

3.5. Material Removal Analysis

The material removal mechanism of concern with the SPF as exposed fine grain Ti-6Al-4V is the depth of cut. Surface profilometer measurements of the depth of cut can be conducted to determine the height difference between the surface treated region and the base material. The depths of the layers removed were plotted as a function of traverse rate to generate Figure 10.

4. CONCLUSIONS

Although a preliminary investigation into the possibility of generating surface textures by using waterjet processes at 600 MPa, the experimental results show that controlled surface texturing can be achieved by controlling the waterjet process parameters. The process parameters can be used to control both the surface roughness and the degree of erosion that occurs due to jet / material interactions. This shows great promise regarding the advancement of controlled 600 MPa waterjet surface preparation processes.

During SPF forming of Ti-6Al-4V, the alpha layer (a brittle layer that is extremely detrimental to the fatigue performance of components) that forms due to high temperatures is approximately 25 micrometers in depth, which is indicated by the red line in Figure 10. The end goal is to remove the boron coating, as well as this brittle alpha layer. The case of a 31.7 mm/s jet traverse rate is very close to achieving the desired removal. It appears that when the jet traverse rate is 31.7 mm/s, approximately 25 micrometers can be removed.

In closing, it has been shown that waterjet processes at 600 MPa provide an alternative means of removing unwanted coatings / materials. In addition, the waterjet brings about the added benefits of inducing compressive residual stresses due to the droplet impact phenomenon. This is an added benefit that alternative coating removal processes (such as chemical milling) do not present. For these reasons, further investigations into the use of UHP waterjet processes for precision surface preparation are highly warranted.

5. ACKNOWLEDGEMENTS

A special thanks to Steve Craigen, of Flow International, for his assistance with the specimen preparation.

6. REFERENCES

- [1] Hashish, M. "Waterjet Cutting at 600 MPa." *BHR Group Symposium of Water Jetting*. 2004, pp. 47 – 60.
- [2] Louis, H., Mohamed, M. and Pude, F. "Cutting Mechanism and Cutting Efficiency for Water Pressures above 600 MPa." *Proceedings of the WJTA American Waterjet Conference*. Paper 1-A. 2003.
- [3] Salko, D. "Peening by Water." *Proceedings of the 2nd International Conference on Shot Peening, ICSP-2*. American Shot Peening Society, NJ. 1984.
- [4] Colosimo, B.M., Monno, M., and Semeraro, Q. "Process parameters control in water jet peening." *International Journal of Materials and Product Technology*. Vol. 15, No. 1/2, 2000, pp. 10-19.
- [5] Kunaporn, S. and Ramulu, M. "Ultra High Pressure Waterjet Peening, Part I: Surface Texture." *Proceedings of the WJTA American Waterjet Conference: Volume 1*, 2001, pp. 90 – 95.
- [6] Kunaporn, S., Ramulu, M., Jenkins, MG, Hashish, M. "Residual stress induced by waterjet peening: A finite element analysis." *Journal of Pressure Vessel Technology*. Vol. 126, No. 3, 2004, pp. 333 – 340.
- [7] Kunaporn, S. "An Experimental and Numerical Analysis of Waterjet Peening of 7075-T6 Aluminum Alloy." Ph.D. Dissertation. University of Washington, 2002.
- [8] Kunaporn, S. and Ramulu, M. and Hashish, M. "Mathematical Modeling of Ultra-High-Pressure Waterjet Peening." *ASME Journal*. Vol. 127, No. 2, 2005, pp. 186 – 191.
- [9] Vikram, G. and Babu, N.R. "An analytical model for prediction of residual stresses in water jet peening." *Proceedings of the WJTA American Waterjet Conference*. Paper 5-A. 2003.
- [10] Ramulu, M., Kunaporn, S., Arola, D., Hashish, M., Hopkins, J. "Waterjet machining and peening of metals." *Journal of Pressure Vessel Technology*, Vol. 122, No. 1, 2000, pp. 90 – 95.

- [11] Ramulu, M., Kunaporn, S., Jenkins, M., Hashish, M., and Hopkins, J. “Fatigue Performance of High-Pressure Waterjet-Peened Aluminum Alloy.” *ASME Journal of Pressure Vessel Technology*. Vol 124, No. 1, 2002, pp. 118 – 123.
- [12] Arola, D., McCain, M.L., Kunaporn, S., Ramulu, M. “Waterjet and abrasive waterjet surface treatment of titanium: a comparison of surface texture and residual stress.” *Wear Journal*. Vol. 249, No.-, 2002, pp. 943 – 950.
- [13] Hashish, M. and Chillman, A. and Ramulu, M. “Waterjet Peening at 600 MPa: A First Investigation.” *Proceedings of the IMECE: 2005 ASME Mechanical Engineering Congress and Exposition*. 2005.
- [14] Chillman, A., Ramulu, M. and Hashish, M. “Waterjet Peening at 600 MPa: An Initial Investigation.” *Journal of Fluids Engineering; ASME*. Vol. 129, Issue 4, pp. 485-490. 2007.

7. TABLES

Table 1. Conditions for Specimen #1 (Experimental Set #1).

Run	Traverse Rate (mm/s)	Lateral Disp. (mm)	D (orifice) (mm)	Pressure (MPa)	Stand Off Distance (mm)	# of passes #
1	21.7	0.2	0.254	600	25.4	8
2	31.7	0.2	0.254	600	25.4	8
3	42.3	0.2	0.254	600	25.4	8
4	84.7	0.2	0.254	600	25.4	8
5	169.3	0.2	0.254	600	25.4	8

Table 2. R_a , R_q , R_y and R_z measurements for Experimental Set #2.

Trav Rate (mm/s)	Measured Direction	R_a (μm)	R_q (μm)	R_y (μm)	R_z (μm)
21.2	Parallel	5.20	6.66	39.11	35.83
31.7	Parallel	0.32	0.41	2.57	2.05
42.3	Parallel	0.33	0.42	2.56	2.05
84.7	Parallel	0.31	0.39	2.19	1.89
169.3	Parallel	0.33	0.43	2.68	2.03
21.2	Perp.	5.63	7.15	28.33	25.39
31.7	Perp.	0.55	0.69	3.98	3.20
42.3	Perp.	0.46	0.58	3.43	2.84
84.7	Perp.	0.52	0.66	3.75	3.18
169.3	Perp.	0.52	0.66	3.90	3.13

8. GRAPHICS

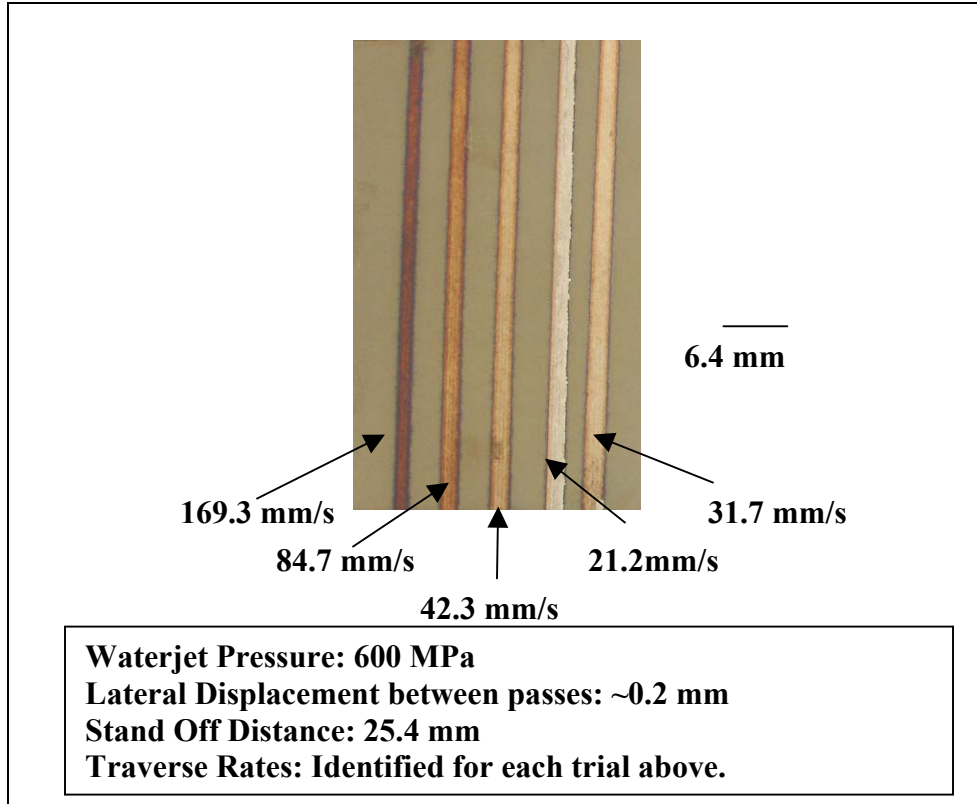


Figure 1. Experimental Set #1 as-prepared.

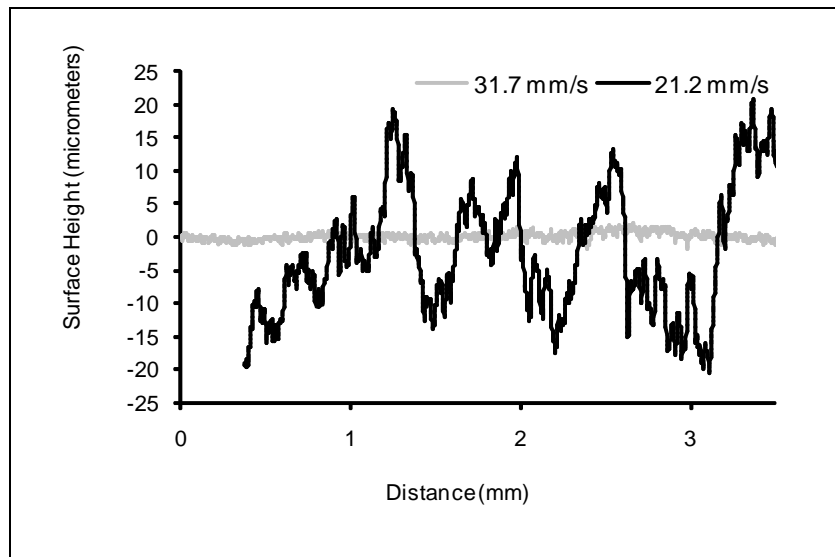


Figure 2. Surface Profiles for 21.2 mm/s and 31.7 mm/s traverse rates.

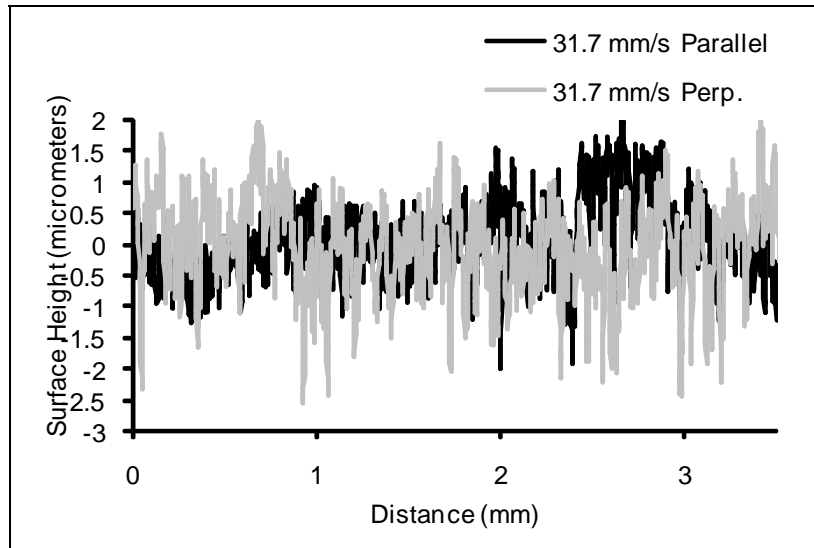


Figure 3. Surface Profiles for 31.7 mm/s parallel and perpendicular to jet traverse.

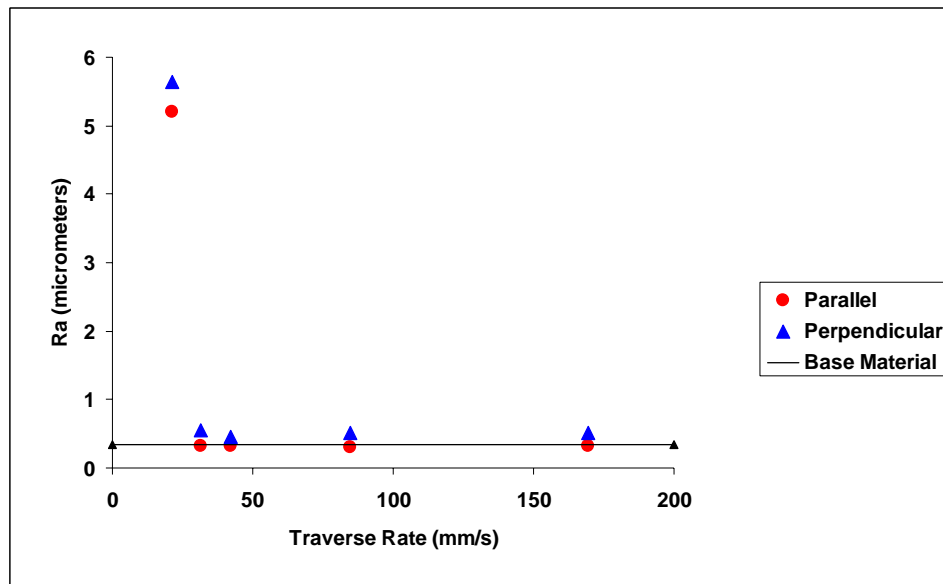


Figure 4. Arithmetic surface roughness (R_a) values for SPF as exposed conditions of Set #2.

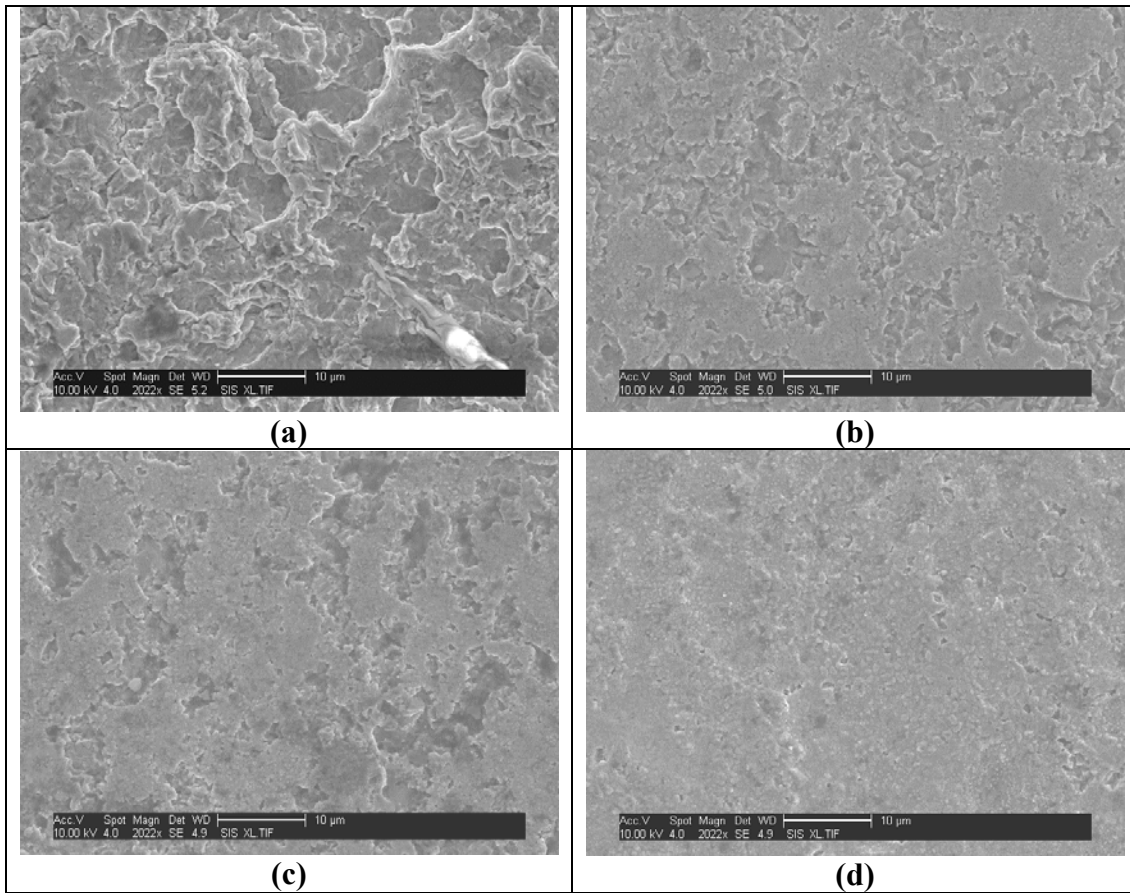


Figure 5. SEM Surface erosion images of SPF Titanium Alloy at 2000x magnification. The traverse speeds are (a) 21.2mm/s (b) 31.7mm/s (c) 42.3 mm/s and (d) 169.3 mm/s.

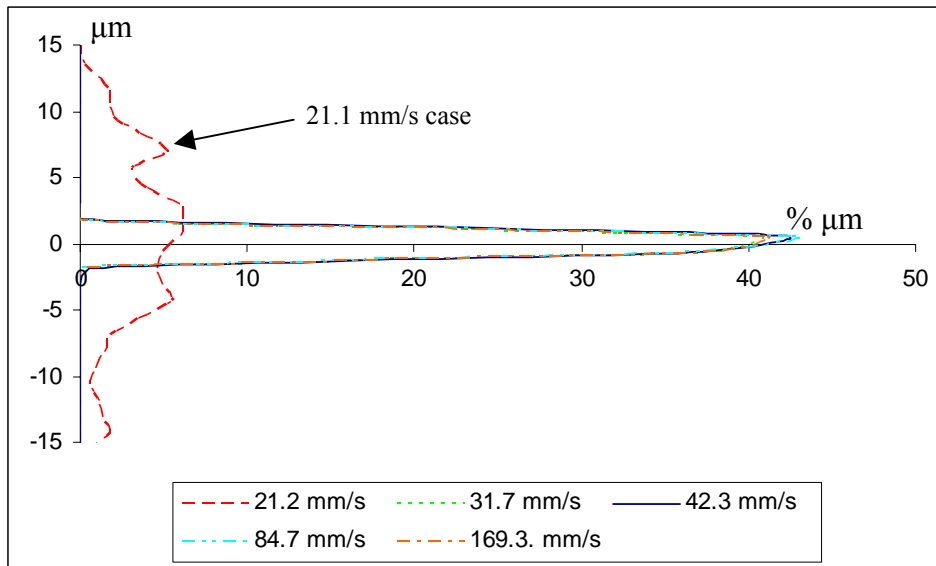


Figure 6. Experimental Set #2 - Profile Height Distributions for Parallel cases.

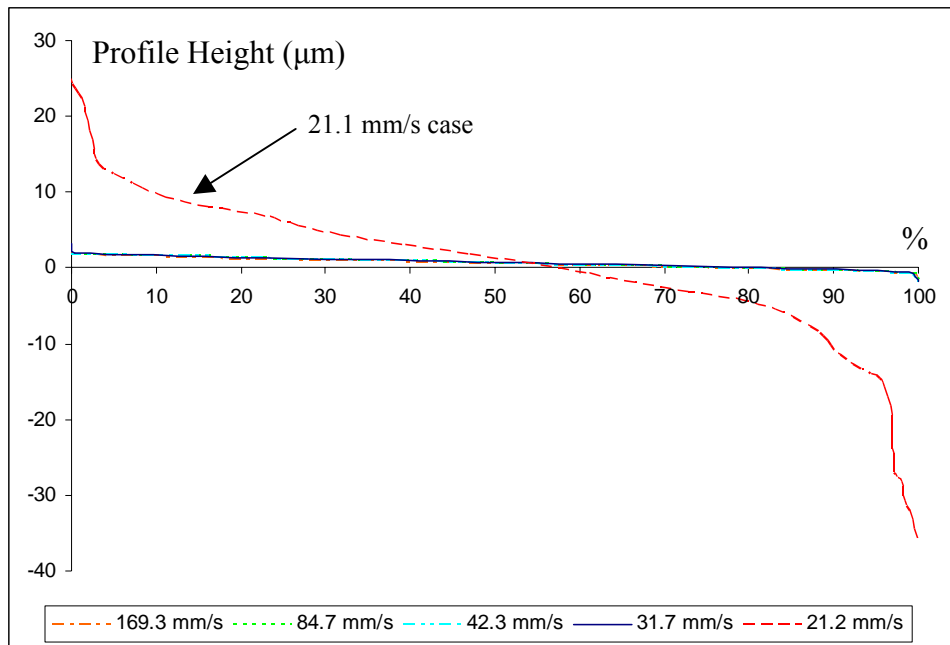


Figure 7. Experimental Set #2 - Bearing Curves.

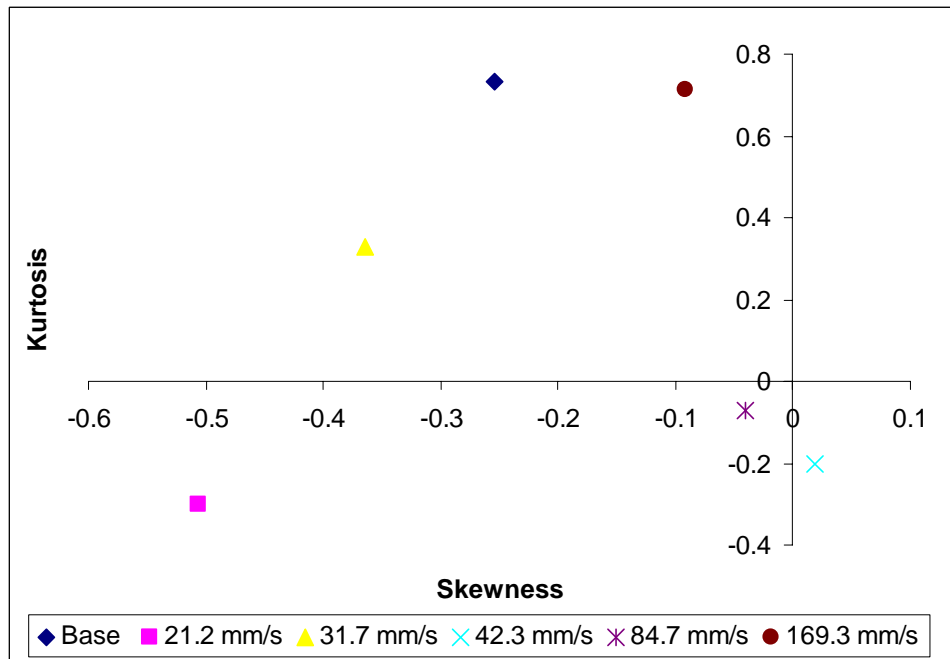


Figure 8. Experimental Set #2 Skewness vs. Kurtosis

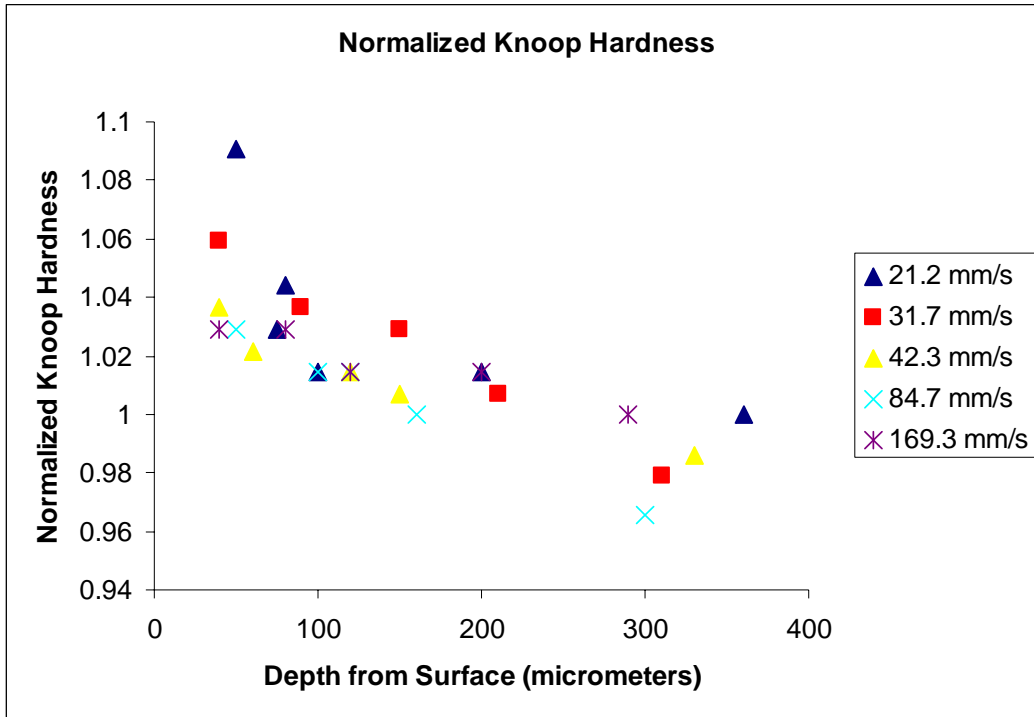


Figure 9. Normalized Knoop micro-hardness evaluation of Set #2. *

*Nominal Knoop Hardness from base material experimentation: 357.9 (as compared to 400 for Ti-6Al-4V according to approximation from Rockwell C value)

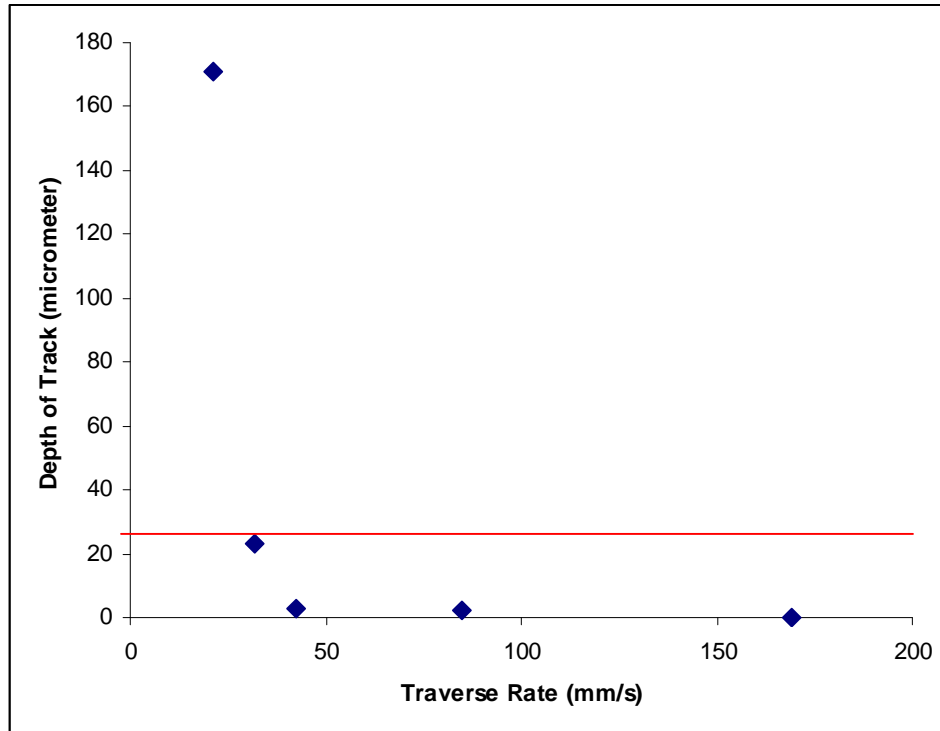


Figure 10. Depth of Cut as a function of jet traverse rate for Experimental Set #2.